



# Relativistic Jet Motion in the Radio-quiet LINER Galaxy KISSR 872

Preeti Kharb<sup>1</sup>, Eric G. Blackman<sup>2,3</sup>, Eric Clausen-Brown<sup>4</sup>, Mousumi Das<sup>5</sup>, Daniel A. Schwartz<sup>6</sup>,  
Aneta Siemiginowska<sup>6</sup>, Smitha Subramanian<sup>5</sup>, and Sravani Vaddi<sup>7</sup>

<sup>1</sup> National Centre for Radio Astrophysics (NCRA) - Tata Institute of Fundamental Research (TIFR), S.P. Pune University Campus, Ganeshkhind, Pune 411007, Maharashtra, India; [kharb@ncra.tifr.res.in](mailto:kharb@ncra.tifr.res.in)

<sup>2</sup> Department of Physics and Astronomy, University of Rochester, Rochester, NY 14627, USA

<sup>3</sup> Laboratory for Laser Energetics, University of Rochester, Rochester, NY 14623, USA

<sup>4</sup> Microsoft, Greater Seattle Area, Washington, USA

<sup>5</sup> Indian Institute of Astrophysics (IIA), II Block, Koramangala, Bangalore 560034, Karnataka, India

<sup>6</sup> Smithsonian Astrophysical Observatory, Cambridge, MA 02138, USA

<sup>7</sup> Arecibo Observatory, NAIC, HC3 Box 53995, Arecibo, PR 00612, USA

Received 2023 November 7; revised 2023 December 12; accepted 2023 December 16; published 2024 February 20

## Abstract

We report superluminal jet motion with an apparent speed of  $\beta_{\text{app}} = 1.65 \pm 0.57$  in the radio-quiet (RQ) low-ionization nuclear emission-line region (LINER) galaxy KISSR 872. This result comes from two-epoch phase-referenced very long baseline interferometry observations at 5 GHz. The detection of bulk relativistic motion in the jet of this extremely radio-faint active galactic nucleus (AGN), with a total 1.4 GHz flux density of 5 mJy in the  $5''.4$  resolution Very Large Array FIRST survey image and 1.5 mJy in the  $\sim 5$  mas resolution Very Long Baseline Array image, is the first of its kind in an RQ LINER galaxy. The presence of relativistic jets in lower accretion rate objects like KISSR 872, with an Eddington ratio of 0.04, reveals that even RQ AGN can harbor relativistic jets and provides evidence of their universality over a wide range of accretion powers.

*Unified Astronomy Thesaurus concepts:* [LINER galaxies \(925\)](#)

## 1. Introduction

A distinguishing characteristic of a radio-loud (RL) active galactic nucleus (AGN) is the presence of relativistic jets. Jets in radio-quiet (RQ) AGN, when present, are typically small, confined to their host galaxies, and slow-moving (Kellermann et al. 1989; Middelberg et al. 2004). Such observational evidence has led to the inference of differing accretion rates and potentially differing accretion disk structures in RL versus RQ AGN. Supermassive black holes (SMBHs;  $M_{\text{BH}} \sim 10^6\text{--}10^9 M_{\odot}$ ) in RL AGN are believed to be powered at high accretion rates (Eddington ratios,  $L_{\text{bol}}/L_{\text{Edd}} > 0.1$ , where  $L_{\text{bol}}$  and  $L_{\text{Edd}}$  are the bolometric and Eddington luminosities, respectively), which leads to optically thick and geometrically thin disks (Shakura et al. 1978; Ho 2008). The SMBHs in RQ AGN, on the other hand, are powered by lower accretion rate disks with  $L_{\text{bol}}/L_{\text{Edd}} < 0.1$  (Ho 2008). These objects could either have  $L_{\text{bol}}/L_{\text{Edd}} \sim \dot{M}/\dot{M}_{\text{Edd}}$ , in which case they would be low-luminosity, high-efficiency accretors and geometrically thin, or  $L_{\text{bol}}/L_{\text{Edd}} \ll \dot{M}/\dot{M}_{\text{Edd}}$ , in which case they would be radiatively inefficient accretion flows (RIAFs; Narayan et al. 1998; Ho 2008; Narayan & McClintock 2008) that are geometrically thick but optically thin. Either way, jets with high bulk relativistic speeds such as typically observed in RL AGN have heretofore not been observed in RQ AGN.

Multiepoch very long baseline interferometry (VLBI) observations of some relatively radio-bright Seyfert galaxies like NGC 1068 and NGC 4258 or RQ quasars like PG 1351+640 and Mrk 231 have detected subrelativistic proper motions with typical jet speeds in the range of  $0.01\text{--}0.5c$  (Peck et al. 2003; Middelberg et al. 2004; Wang et al. 2021, 2023).

On the other hand, VLBI observations of RL AGN like blazars (e.g., from the MOJAVE<sup>8</sup> sample; Lister et al. 2019) reveal apparent jet speeds in the range  $0.05\text{--}35c$ . Doppler boosting effects and superluminal motion are a direct consequence of these bulk relativistic jet effects prompting the revised classification of “jetted” and “nonjetted” AGN in lieu of the RL/RQ divide (Padovani et al. 2017).

In this paper, we present second-epoch VLBI observations of the parsec-scale jet in the RQ type 2 LINER<sup>9</sup> galaxy KISSR 872, which reveals superluminal jet motion. This makes KISSR 872 the only RQ (Section 3) LINER galaxy so far to exhibit bulk relativistic motion in its jet. Furthermore, this result directly challenges the physical equivalence of jetted/nonjetted AGN classification with the RL/RQ classification.

### 1.1. The KISSR Sample: A VLBI Study

We identified nine nearby (redshifts  $z \sim 0.03\text{--}0.09$ ) type 2 Seyfert and LINER galaxies from the KISSR<sup>10</sup> sample of emission-line galaxies (Wegner et al. 2003) that showed double-peaked or asymmetric narrow emission lines in their SDSS<sup>11</sup> optical spectra and were detected in the Very Large Array (VLA) FIRST<sup>12</sup> survey with a total flux density of  $\gtrsim 2$  mJy at 1.4 GHz (Kharb et al. 2015, 2021) in order to carry out a VLBI study. We acquired milliarcsecond-resolution phase-referenced data on these sources at 1.5 and 5 GHz with the Very Long Baseline Array (VLBA) from 2013 to 2019. These data revealed one-sided radio jets in five of the eight (>60%) VLBA-detected sources (Kharb et al. 2021) and dual parsec-scale radio cores in one of them (KISSR 102;

<sup>8</sup> Monitoring Of Jets in Active galactic nuclei with VLBA Experiments.

<sup>9</sup> Low-ionization nuclear emission-line region (Heckman 1980).

<sup>10</sup> KPNO Internal Spectroscopic Survey Red.

<sup>11</sup> Sloan Digital Sky Survey.

<sup>12</sup> Faint Images of the Radio Sky at Twenty cm.

**Table 1**  
VLBA Component Properties in 5 GHz Images

Date	Comp.	R.A. (h m s)	Decl. (deg arcmin arcsec)	$\theta_{\text{maj}}$ (mas)	$\theta_{\text{min}}$ (mas)	PA (deg)	$I_{\text{peak}}$ ( $\mu\text{Jy beam}^{-1}$ )	$S_{\text{total}}$ ( $\mu\text{Jy}$ )
(1)	(2)	(3)	(4)	(5)	(6)	(7)	(8)	(9)
2022 Nov 05	C	15 50 09.805578 $\pm$ 0.000004	29 11 07.2301 $\pm$ 0.0001	4.7 $\pm$ 0.3	2.1 $\pm$ 0.1	174 $\pm$ 3	334.09 $\pm$ 22.1	471.93 $\pm$ 48.6
	X	15 50 09.805743 $\pm$ 0.00001	29 11 07.2316 $\pm$ 0.0003	4.2 $\pm$ 0.7	2.3 $\pm$ 0.4	169 $\pm$ 11	123.88 $\pm$ 22.2	167.76 $\pm$ 47.4
	J0	15 50 09.806027 $\pm$ 0.00001	29 11 07.2380 $\pm$ 0.0003	5.2 $\pm$ 0.9	2.7 $\pm$ 0.5	161 $\pm$ 10	121.23 $\pm$ 21.5	239.93 $\pm$ 60.4
2018 Dec 31	C	15 50 09.805569 $\pm$ 0.000003	29 11 07.22982 $\pm$ 0.00008	3.6 $\pm$ 0.2	2.0 $\pm$ 0.1	179 $\pm$ 4	299.01 $\pm$ 17.2	303.90 $\pm$ 30.2
	J0	15 50 09.805944 $\pm$ 0.000007	29 11 07.2370 $\pm$ 0.0001	3.9 $\pm$ 0.4	2.1 $\pm$ 0.2	170 $\pm$ 6	160.34 $\pm$ 17.1	192.23 $\pm$ 33.5

**Note.** Column (1) notes the dates of the 5 GHz VLBA observations. Column (2) indicates the VLBA components in the 5 GHz images as shown in Figure 1. Columns (3)–(4) note the component positions in R.A. and decl. as provided by the Gaussian-fitting AIPS task JMFIT. Columns (5)–(7) provide the major and minor axes of the fitted Gaussian components in milliarcseconds along with their position angles in degrees. Column (8) notes the peak surface brightness, while column (9) lists the total flux density at 5 GHz.

Kharb et al. 2020). Based on the jet-to-counterjet surface brightness ratios, we obtained limits on the parsec-scale jet speeds assuming jet inclination angles of  $\geq 50^\circ$ , as these were type 2 AGN, and the half-opening angle of the dusty obscuring torus has been suggested to be  $\sim 50^\circ$  (Simpson et al. 1996). Type 2 AGN are those with narrow emission lines in their spectra, as the broad lines are expected to be hidden behind an obscuring dusty torus (Antonucci 1993).

This treatment assumes that the jet one-sidedness is a consequence of Doppler boosting/deboosting effects in approaching/receding jets in these RQ AGN, similar to those in RL AGN. This exercise revealed a range of jet speeds from 0.003 to 0.75 $c$  in the KISSR galaxies (larger inclination angles would imply larger intrinsic jet speeds). Interestingly, this speed range is broadly consistent with apparent jet speeds measured in a handful of radio-bright Seyfert galaxies through multiepoch VLBI observations (Roy et al. 2001; Peck et al. 2003; Middelberg et al. 2004). While one-sided jets could also arise due to free-free absorption by the intercloud gas in the narrow-line regions (NLRs; Kharb et al. 2021), this cannot be a favored explanation for jets that are 150 pc (KISSR 434; Kharb et al. 2019) or 200 pc (KISSR 872; Kharb et al. 2021) long.

KISSR 872 is a type 2 LINER galaxy at a redshift of 0.08255.<sup>13</sup> It has a peak intensity at 1.4 GHz of  $4.80 \pm 0.15$  mJy beam $^{-1}$  and a total flux density of  $5.25 \pm 0.27$  mJy in the VLA FIRST survey ( $\theta = 5''.4$ ). In this paper, the spectral index  $\alpha$  is defined such that flux density at a frequency  $\nu$ ,  $S_\nu \propto \nu^\alpha$ . The adopted cosmology is  $H_0 = 67.8$  km s $^{-1}$  Mpc $^{-1}$ ,  $\Omega_{\text{mat}} = 0.308$ , and  $\Omega_{\text{vac}} = 0.692$ , so that at the distance of KISSR 872, 1'' corresponds to 1.608 kpc.

## 2. Radio Data Analysis

VLBI observations were carried out in a phase-referencing mode using eight antennas of the VLBA at 1.5 GHz on 2022 September 13 (Project ID: BK246A2); the Kitt Peak (KP) and Pie Town antennas did not participate in the experiment for technical reasons. Observations at 5 GHz were carried out on 2022 November 5 (Project ID: BK246B4) with nine antennas of the VLBA; KP did not participate in this experiment for technical reasons. For both of these data sets, 3C 345 was used as the fringe finder, while the nearby calibrator 1537+279 was used as the phase-referencing source. The positional errors in the X- and Y-directions for 1537+279 were 0.35 and 0.81 mas,

and the separation from KISSR 872 was  $2''.72$ . The target and the phase reference calibrator were observed in a “nodding” mode in a 5 minute cycle (2 minutes on calibrator and 3 minutes on source) for good phase calibration.

The data were processed using the VLBA data calibration pipeline procedure VLBARUN<sup>14</sup> in the Astronomical Image Processing System (AIPS; Greisen 2003). VLBARUN is based on the VLBAUTIL procedures; their step-by-step usage is described in Appendix C of the AIPS Cookbook.<sup>15</sup> The Los Alamos antenna was used as the reference antenna for both data sets. The source images were not self-calibrated. All images were created using uniform weighting with ROBUST +5. The resultant rms noise in the images was  $\sim 30$   $\mu\text{Jy beam}^{-1}$  at 1.5 GHz and  $\sim 20$   $\mu\text{Jy beam}^{-1}$  at 5 GHz. The component positions and flux densities along with errors were obtained with the AIPS Gaussian-fitting task JMFIT (see Table 1). JMFIT estimates the errors in the Gaussian model fits as a function (inverse square root) of the component surface brightness, as described by Condon (1997). We note that these errors dominate over the astrometric errors due to the VLBA phase-referencing process, which at the decl. of KISSR 872 is  $\leq 50$   $\mu\text{arcsec}$  (Pradel et al. 2006).

We created the 1.5–5 GHz spectral index image for KISSR 872 by first matching the UV-spacing at both frequencies by fixing the UVTAPER parameter to 0–50 mega $\lambda$  and creating both images with a synthesized beam equal to that of the lower-frequency image ( $11.01 \times 4.28$  mas, PA =  $7^\circ.3$ ). The “core” positions were made coincident using the AIPS task OGEOM before using the AIPS task COMB to create the spectral index image. Pixels with flux density values below three times the rms noise were blanked in COMB. A spectral index noise image was created as well. The spectral index and noise values are reported in Section 3.

## 3. Results

We detect a bright compact component (core, or C) and a jet component (J0) in our VLBA 5 GHz image from 2022 November 5 (see Figure 1), similar to the VLBA 5 GHz image from 2018 December 31. In addition, we see the birth of a new jet component from the core (noted as X in Figure 1). The positions of these components from the two epochs are noted in Table 1. The identification of component C as the core is based on both its relative brightness and its stationarity (with an

<sup>13</sup> From the SDSS Data Release 13 as obtained on 2017 January 31 and listed in the NASA/IPAC Extragalactic Database.

<sup>14</sup> URL: <http://www.aips.nrao.edu/vlbarun.shtml>

<sup>15</sup> URL: <http://www.aips.nrao.edu/cook.html>

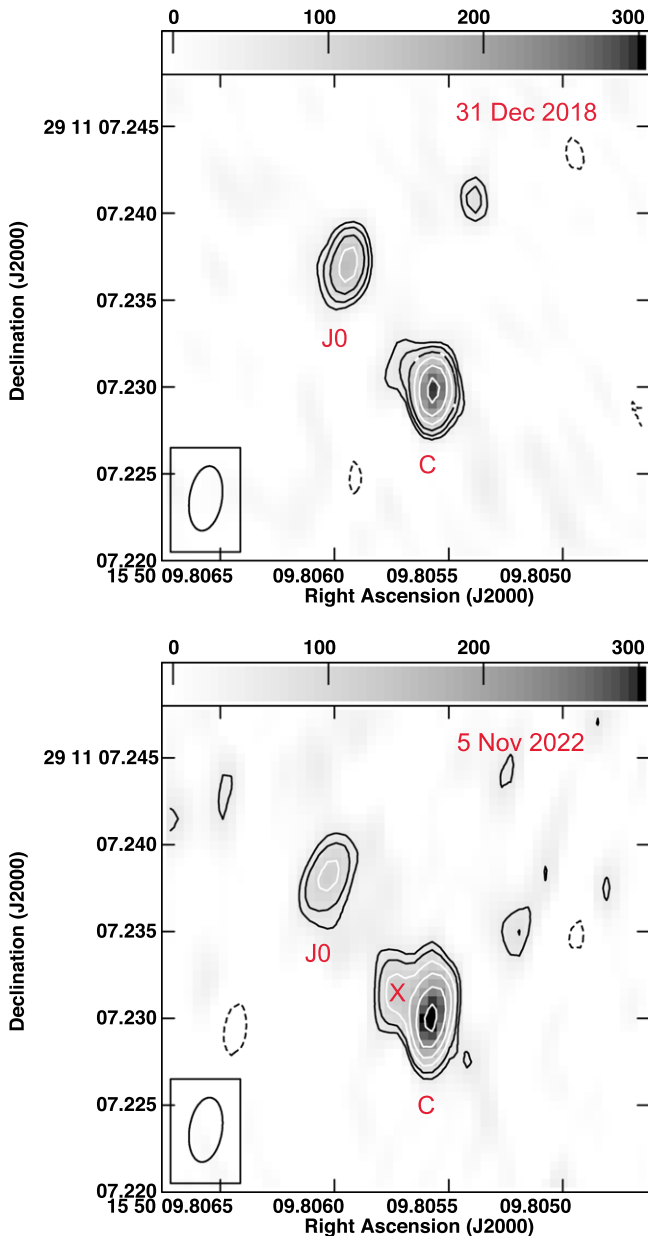


**Figure 1.** VLBA image at 5 GHz in contours and gray scale (top) from 2018 December 31 with contour levels  $2.962 \times (-16, 16, 22.50, 32, 45, 64, 90) \mu\text{Jy beam}^{-1}$  and (bottom) from 2022 November 5 with contour levels  $3.410 \times (-16, 16, 22.50, 32, 45, 64, 90) \mu\text{Jy beam}^{-1}$ . The gray scale ranges from 1.5 to 301.5  $\mu\text{Jy beam}^{-1}$  in both panels. The beam is  $3.75 \times 1.87$  mas at a PA =  $-8^\circ 8'$  in both panels.

uncertainty of 90–130  $\mu\text{as}$  in the two epochs). It is worth noting here that relatively steep-spectrum VLBI “cores,” as was observed in the previous epoch for KISSR 872, have been observed in other RQ AGN as well (e.g., Roy et al. 2000; Orienti & Prieto 2010; Bontempi et al. 2012; Panessa & Giroletti 2013).

The C–J0 distance changes from  $8.7 \pm 0.2$  mas ( $14.0 \pm 0.3$  pc) to  $9.8 \pm 0.4$  mas ( $15.8 \pm 0.6$  pc) over this time period (time = 121.392 Ms). For a time dilation factor of 1.08255 in the source frame, we measure the apparent speed of the jet component J0 to be  $\beta_{\text{app}} = 1.65 \pm 0.57$ . If we assume the bulk flow speed to be  $c$ , then we can derive a maximum possible viewing angle for the jet components with  $\beta_{\text{app}} = 1.65$  as  $62^\circ$ . We also estimate the jet-to-counterjet intensity ratio,  $R_J$ , in the

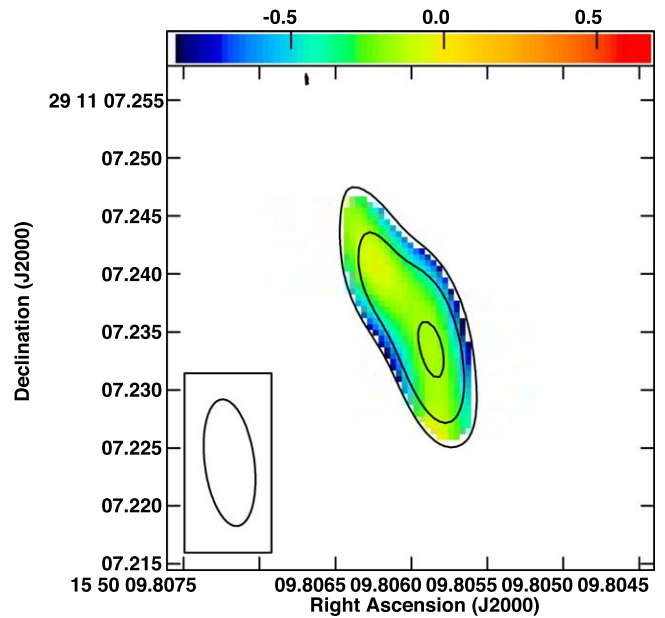


**Figure 2.** The 1.5–5 GHz spectral index image from 2022 in color superimposed by 5 GHz contours at levels  $4.77 \times (22.5, 45, 90) \mu\text{Jy beam}^{-1}$ . The beam is  $11.01 \times 4.28$  mas at a PA =  $7^\circ 3'$ .

new 5 GHz image to be  $>2.1$ , where three times the rms noise is considered as an upper limit to the counterjet emission. For  $\beta=1$ , a jet inclination of  $<83^\circ$  would be implied for a jet structural parameter,  $p$ , of 3. These inclination angles are consistent with the type 2 classification of KISSR 872.

The 1.5 GHz VLBA image from 2022 September shows the “core” structure to have evolved drastically compared to the 2019 January VLBA data (see Figures 2 and 3). The 1.5–5 GHz spectral index image reveals the average core–jet region spectral index to be  $-0.31 \pm 0.19$ , which is also substantially flatter than the average value of  $-0.71 \pm 0.26$  derived in 2019 January (Kharb et al. 2021). One mechanism that can explain the spectral index flattening would be the emergence of a free-free emitting wind component along with the synchrotron jet in the intervening period of 4 yr (see the two panels in Figure 3). This would give credence to the suggestion of a dynamically changing jet+wind structure being present in Seyfert and LINER outflows (Nevin et al. 2018; Kharb & Silpa 2023). Magnetically collimated jets require a bounding pressure to stabilize and confine the fields (e.g., Begelman et al. 1984; Lynden-Bell 1996). There do not seem to be any astrophysical jet sources where a bounding envelope or wind is proven to be absent (Blackman & Lebedev 2022).

In the 1.5 GHz image, we detect a  $\sim 3.6\sigma$  feature close in position to the jet component J2 as reported in Kharb et al. (2021; marked as “J2?” in Figure 4). If this is the same feature as J2, the inferred jet speed would be unusually large at  $\sim 13c$ . Given the faintness of this feature, however, additional data are needed to determine the true nature of this component. Nevertheless, on the basis of the high signal-to-noise ratio detection of components C and J0 in the 5 GHz images from two epochs, we conclude that KISSR 872 is the first RQ LINER galaxy to show superluminal jet motion in its parsec-scale jet.

Using the [O III]  $\lambda 5007$  line luminosity and the relation from Heckman et al. (2004), the bolometric luminosity ( $L_{\text{bol}}$ ) in KISSR 872 is  $2.3 \times 10^{44} \text{ erg s}^{-1}$ . A black hole mass of  $4.4 \times 10^7 M_\odot$  has

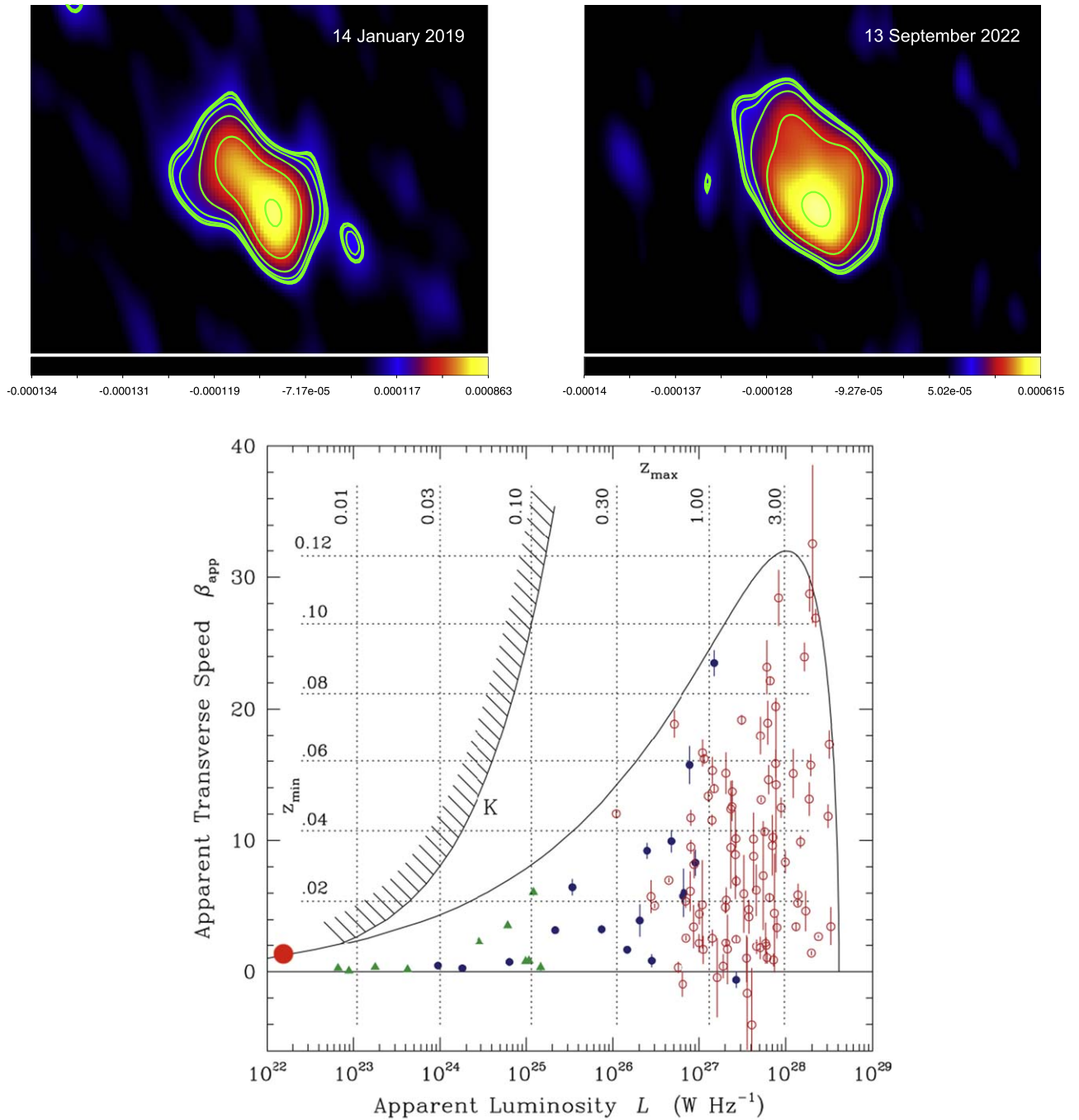


**Figure 3.** VLBA image at 1.5 GHz in contours and color with the contour levels being (for top left panel from 2019 January 14) at 95.00, 96.42, 100.89, 115.06, 159.84, 301.47, and 749.34  $\mu\text{Jy beam}^{-1}$  and (for top right panel from 2022 September 13) at 95.00, 95.87, 98.64, 107.40, 135.09, 222.67, and 499.59  $\mu\text{Jy beam}^{-1}$ . The bottom panel shows the position of KISSR 872 as a filled red circle in the speed–luminosity plot of Cohen et al. (2007) for the 2 cm VLBA survey sources.

been estimated in KISSR 872 using the stellar velocity dispersion ( $\sigma$ ) from spectral line fitting and the  $M_{\text{BH}}-\sigma$  relation from McConnell & Ma (2013). The Eddington luminosity ( $\equiv 1.25 \times 10^{38} M_{\text{BH}}/M_{\odot}$ ) is  $5.6 \times 10^{45} \text{ erg s}^{-1}$ , and the Eddington ratio is 0.04. Its radio-to-optical luminosity ratio,  $R = L(5 \text{ GHz})/L(4858 \text{ \AA}) = 1.59 \times 10^{22}/6.17 \times 10^{21} [\text{W/Hz}] = 2.6$ , places it firmly in the RQ AGN category. Here we have used nuclear AGN properties (see Ho 2008) by using the VLBI 5 GHz luminosity and the SDSS  $g$ -band “PSF” luminosity from the NASA/IPAC Extragalactic Database, the  $g$  band being the closest in wavelength to the  $B$  band used in the original work of

Kellermann et al. (1989). Finally, the jet power,  $Q_{\text{jet}}$ , of  $2.6 \times 10^{43} \text{ erg s}^{-1}$  is estimated using the 5 GHz radio luminosity,  $L_{\text{R}} = 8.0 \times 10^{38} \text{ erg s}^{-1}$ , and the relativistic beaming-corrected relations of Merloni & Heinz (2007). Interestingly, this value lies in the range of  $Q_{\text{jet}}$  values estimated for RL FR I radio galaxies (Rawlings & Saunders 1991).

#### 4. Discussion

A jet speed of  $\sim 1.25\text{--}2.66c$  has been detected in the Seyfert 2 galaxy III Zw 2 (Brunthaler et al. 2000). However, III Zw 2 is a radio-intermediate AGN with  $\sim 50 \text{ kpc}$  ( $\sim 30 \text{ kpc}$  on one side)

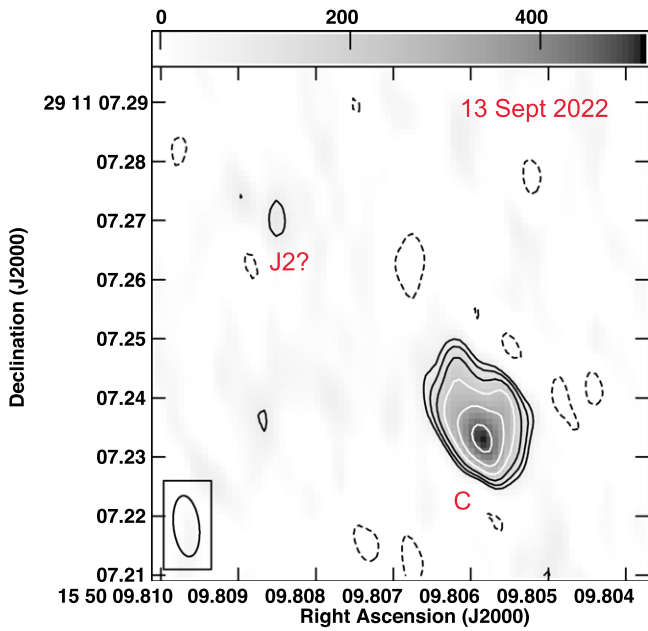


**Figure 4.** VLBA image at 1.5 GHz in contours and gray scale from 2022 September 13. The contour levels are  $5.055 \times (-16, 16, 22.50, 32, 45, 64, 90) \mu\text{Jy beam}^{-1}$ . The gray scale ranges from  $-2.5$  to  $508 \mu\text{Jy beam}^{-1}$ . Component C is the core region, while component J2 is as noted in the 2019 January data presented in Kharb et al. (2021). The beam is  $10.34 \times 4.35$  mas at a PA =  $6^\circ 5$ .

jets (Silpa et al. 2021). The production of jets in AGN likely requires magnetically mediated extraction of energy and angular momentum from either a fast-rotating SMBH via the Blandford & Znajek (1977) mechanism, a magnetic tower from field lines linking the accretion disk and the black hole (Lynden-Bell 1996), a jet anchored in the surrounding accretion disk (Blandford & Payne 1982), or some combination of these that evolves in time (e.g., Sikora & Begelman 2013). The magnetic jet must also itself be stabilized by a surrounding pressure. The presence of a magnetically arrested disk (MAD; Narayan et al. 2003) with outflows driven by the Blandford & Znajek (1977) mechanism has been invoked to explain collimated and highly magnetized jets in RL AGN. While this may dominate for RL sources, the VLBI core-shift study of Chamani et al. (2021) reports that the magnetic field strength limits derived for III Zw 2, with the caveat that “equipartition” between magnetic and particle energy is assumed, are too small for an MAD to be operational. This does not, however, preclude a magnetically mediated jet.

The RQ quasar Mrk 231 typically exhibits subrelativistic jet speeds in the range of  $0.013$ – $0.14c$  (Ulvestad et al. 1999; Wang et al. 2021) but can turn superluminal ( $v > 3.15c$ ) during flaring states (Reynolds et al. 2017). Similarly, a three-epoch VLBI monitoring study of the RQ quasar PG 1351+640 by Wang et al. (2023) shows a sudden increase in its jet speed over the recent two epochs, even though its overall speed remains subrelativistic at  $0.37c$ . Such behavior (of varying speeds for individual jet knots over time) is also observed in the long-term VLBI monitoring studies of RL blazars (e.g., Cohen et al. 2007), underscoring the importance of continuous VLBI monitoring of AGN jets to fully understand their nature. Sbarrato et al. (2021) have highlighted the case of relativistic jets in two high-redshift ( $z > 5$ ) RQ quasars, viz, SDSS J0100+2802 and SDSS J0306+1853, based on spectral energy

distribution (SED) modeling and suggested that relativistic jets may be more common in the early Universe.

The case of KISSR 872 exemplifies that relativistic jets can persist in lower accretion rate engines. Their jets may benefit from having phases of a thick-disk mode of accretion (Rees et al. 1982; Lynden-Bell 2003; Sikora & Begelman 2013), as would be the case with an RIAF, although we cannot know if this source is an RIAF without an independent estimate of the accretion rate. A thick disk can help supply large-scale flux and may also help to collimate a jet from the central black hole, but a broad wind pressure confining a magnetic jet from a thin disk is also possible. The maximum four-velocity of the jet in typical models is determined by the product of the angular speed at which the footpoints are anchored times the radius out to which field lines remain quasi-rigid, i.e., the Alfvén radius (Blandford & Königl 1979; Blandford & Payne 1982; Pelletier & Pudritz 1992; Lynden-Bell 2003). That can be relativistic even for a modest magnetic field if the black hole is spinning rapidly. The extent to which the disk versus the black hole is the predominant anchoring rotator for a jet’s magnetic field in intermediate and weak radio sources is not well constrained, as a faster-spinning black hole would also mean a closer innermost stable orbit of the disk. Only for jets so powerful that they exceed the available accretion power is extraction from the black hole essential, but this is not the case for KISSR 872.

It is worth noting that, using optical/UV (o) and X-ray (x) data on LINER galaxies, Maoz (2007) concluded that there may be no sharp changes in the source SEDs at the lowest luminosities; thin AGN accretion disks could persist at low accretion rates. Using the Maoz (2007) LINER sample, Sobolewska et al. (2011) showed that the  $\alpha_{\text{ox}}$  values of LINERs were consistent with their accretion disks being in a hard spectral state, a state that produces jets, analogous to the case of Galactic X-ray binaries.

Interestingly, KISSR 872 falls close to the “aspect curve” generated by Cohen et al. (2007) for an intrinsic Lorentz factor of 32 and an intrinsic luminosity of  $10^{25} \text{ W Hz}^{-1}$ , which envelopes the apparent transverse speed and (15 GHz) radio luminosity data for RL AGN belonging to the 2 cm VLBA survey (Kellermann et al. 1998). These data support the idea that the “relativistic beaming model” works for the entire population of 2 cm VLBA sources and perhaps also KISSR 872. In the case of KISSR 872, the 15 GHz apparent radio luminosity ( $L = 1.2 \times 10^{22} \text{ W Hz}^{-1}$ ) was estimated using the VLBA 5 GHz total flux density assuming  $\alpha = -0.3$ . This result highlights the universality of jets over a wide range of accretion and radio powers and raises questions about the presence of intrinsically different central engines in RL and RQ AGN. The reduced spread in superluminal speeds of the low-luminosity sources would be consistent with lower Lorentz factors of the jet at the loci of observation and thus a need to be more favorably inclined close to the inclination angle to the observer that maximizes the apparent jet speed.

## 5. Summary and Conclusions

We report the detection of superluminal jet motion and thereby the presence of a relativistic jet in the RQ LINER galaxy KISSR 872. Unlike the other Seyfert galaxy showing superluminal jet motion, viz, III Zw 2, which has  $\sim 50$  kpc jets and is largely a radio-intermediate AGN, any kiloparsec-scale outflow in KISSR 872 is  $\leq 8.7$  kpc in extent, that being the







resolution of the VLA FIRST image ( $\theta = 5''4$ ). Moreover, only 5 mJy of the radio flux density is present within this 8.7 kpc region at 1.4 GHz, 44% of which is present in the 200 pc-scale region probed by the VLBA (see Kharb et al. 2021), making this an extremely RQ AGN. The results from our VLBI study of KISSR 872 demonstrate that its engine can produce relativistic jets that can influence the NLR clouds giving rise to double-peaked emission lines in its optical spectra. The presence of relativistic jets in an extremely RQ AGN like KISSR 872 also challenges any suggestion of intrinsically different central engines in RQ AGN compared to RL AGN and highlights the universality of jets over a wide range of accretion powers. The position of KISSR 872 in the ( $\beta_{\text{app}}$ ,  $L$ ) plot of RL AGN by Cohen et al. (2007) is consistent with these suggestions. The conclusion for black hole engines resonates with similar conclusions reached for disk-jet sources from nonrelativistic engines like protostars (Narang et al. 2023). It remains to be determined what engine geometry, and thus the exact mechanism of jet collimation, is operating in a low-luminosity AGN like KISSR 872.

### Acknowledgments

We thank the referee for a careful reading of our manuscript and providing us with suggestions that have improved the manuscript significantly. We thank Zsolt Paragi for the insightful suggestions that have improved this manuscript. P.K. acknowledges the support of the Department of Atomic Energy, Government of India, under project 12-R&D-TFR-5.02-0700. P.K. acknowledges the support of the Chandra X-ray Center and the Center for Astrophysics, Harvard & Smithsonian, as a visiting scientist. M.D. acknowledges the support of Science and Engineering Research Board (SERB) grant CRG/2022/004531 for this research. A.S. and D.A.S. are supported by NASA contract NAS8-03060 to the Chandra X-ray Center of the Smithsonian Astrophysical Observatory. E.B. acknowledges support from National Science Foundation grant PHY-2020249. The National Radio Astronomy Observatory is a facility of the National Science Foundation operated under cooperative agreement by Associated Universities, Inc. Funding for the Sloan Digital Sky Survey has been provided by the Alfred P. Sloan Foundation, the Heising-Simons Foundation, the National Science Foundation, and the Participating Institutions. SDSS acknowledges support and resources from the Center for High-Performance Computing at the University of Utah. The SDSS website is [www.sdss.org](http://www.sdss.org). This research has made use of the NASA/IPAC Extragalactic Database (NED), which is operated by the Jet Propulsion Laboratory, California Institute of Technology, under contract with the National Aeronautics and Space Administration.

*Facilities:* VLBA, Sloan.

### ORCID iDs

Preeti Kharb  <https://orcid.org/0000-0003-3203-1613>  
 Eric G. Blackman  <https://orcid.org/0000-0002-9405-8435>  
 Eric Clausen-Brown  <https://orcid.org/0000-0003-0260-3561>  
 Mousumi Das  <https://orcid.org/0000-0001-8996-6474>  
 Daniel A. Schwartz  <https://orcid.org/0000-0001-8252-4753>  
 Aneta Siemiginowska  <https://orcid.org/0000-0002-0905-7375>

Smitha Subramanian  <https://orcid.org/0000-0002-5331-6098>

Sravani Vaddi  <https://orcid.org/0000-0003-3295-6595>

### References

- Antonucci, R. 1993, *ARA&A*, **31**, 473  
 Begelman, M. C., Blandford, R. D., & Rees, M. J. 1984, *RvMP*, **56**, 255  
 Blackman, E. G., & Lebedev, S. V. 2022, *NewAR*, **95**, 101661  
 Blandford, R. D., & Königl, A. 1979, *ApJ*, **232**, 34  
 Blandford, R. D., & Payne, D. G. 1982, *MNRAS*, **199**, 883  
 Blandford, R. D., & Znajek, R. L. 1977, *MNRAS*, **179**, 433  
 Bontempi, P., Giroletti, M., Panessa, F., Orienti, M., & Doi, A. 2012, *MNRAS*, **426**, 588  
 Brunthaler, A., Falcke, H., Bower, G. C., et al. 2000, *A&A*, **357**, L45  
 Chamani, W., Savolainen, T., Hada, K., & Xu, M. H. 2021, *A&A*, **652**, A14  
 Cohen, M. H., Lister, M. L., Homan, D. C., et al. 2007, *ApJ*, **658**, 232  
 Condon, J. J. 1997, *PASP*, **109**, 166  
 Greisen, E. W. 2003, in *Information Handling in Astronomy - Historical Vistas*, ed. A. Heck (Dordrecht: Kluwer), 109  
 Heckman, T. M. 1980, *A&A*, **87**, 152  
 Heckman, T. M., Kauffmann, G., Brinchmann, J., et al. 2004, *ApJ*, **613**, 109  
 Ho, L. C. 2008, *ARA&A*, **46**, 475  
 Kellermann, K. I., Sramek, R., Schmidt, M., Shaffer, D. B., & Green, R. 1989, *AJ*, **98**, 1195  
 Kellermann, K. I., Vermeulen, R. C., Zensus, J. A., & Cohen, M. H. 1998, *AJ*, **115**, 1295  
 Kharb, P., Das, M., Paragi, Z., Subramanian, S., & Chitta, L. P. 2015, *ApJ*, **799**, 161  
 Kharb, P., Lena, D., Paragi, Z., et al. 2020, *ApJ*, **890**, 40  
 Kharb, P., & Silpa, S. 2023, *Galax*, **11**, 27  
 Kharb, P., Subramanian, S., Das, M., Vaddi, S., & Paragi, Z. 2021, *ApJ*, **919**, 108  
 Kharb, P., Vaddi, S., Sebastian, B., et al. 2019, *ApJ*, **871**, 249  
 Lister, M. L., Homan, D. C., Hovatta, T., et al. 2019, *ApJ*, **874**, 43  
 Lynden-Bell, D. 1996, *MNRAS*, **279**, 389  
 Lynden-Bell, D. 2003, *MNRAS*, **341**, 1360  
 Maoz, D. 2007, *MNRAS*, **377**, 1696  
 McConnell, N. J., & Ma, C.-P. 2013, *ApJ*, **764**, 184  
 Merloni, A., & Heinz, S. 2007, *MNRAS*, **381**, 589  
 Middelberg, E., Roy, A. L., Nagar, N. M., et al. 2004, *A&A*, **417**, 925  
 Narang, M., Manoj, P., Tyagi, H., et al. 2023, arXiv:2310.14061  
 Narayan, R., Igumenshchev, I. V., & Abramowicz, M. A. 2003, *PASJ*, **55**, L69  
 Narayan, R., Mahadevan, R., & Quataert, E. 1998, in *Theory of Black Hole Accretion Disks*, ed. M. A. Abramowicz, G. Björnsson, & J. E. Pringle (Cambridge: Cambridge Univ. Press), 148  
 Narayan, R., & McClintock, J. E. 2008, *NewAR*, **51**, 733  
 Nevin, R., Comerford, J. M., Müller-Sánchez, F., Barrows, R., & Cooper, M. C. 2018, *MNRAS*, **473**, 2160  
 Orienti, M., & Prieto, M. A. 2010, *MNRAS*, **401**, 2599  
 Padovani, P., Alexander, D. M., Assef, R. J., et al. 2017, *A&ARv*, **25**, 2  
 Panessa, F., & Giroletti, M. 2013, *MNRAS*, **432**, 1138  
 Peck, A. B., Henkel, C., Ulvestad, J. S., et al. 2003, *ApJ*, **590**, 149  
 Pelletier, G., & Pudritz, R. E. 1992, *ApJ*, **394**, 117  
 Pradel, N., Charlot, P., & Lestrade, J. F. 2006, *A&A*, **452**, 1099  
 Rawlings, S., & Saunders, R. 1991, *Natur*, **349**, 138  
 Rees, M. J., Begelman, M. C., Blandford, R. D., & Phinney, E. S. 1982, *Natur*, **295**, 17  
 Reynolds, C., Punsly, B., Miniutti, G., O'Dea, C. P., & Hurley-Walker, N. 2017, *ApJ*, **836**, 155  
 Roy, A. L., Ulvestad, J. S., Wilson, A. S., et al. 2000, in *Perspectives on Radio Astronomy: Science with Large Antenna Arrays*, ed. M. P. van Haarlem (Dwingeloo: NFRA), 173  
 Roy, A. L., Wrobel, J. M., Wilson, A. S., et al. 2001, in *IAU Symp. 205, Galaxies and Their Constituents at the Highest Angular Resolutions*, ed. R. T. Schilizzi et al. (San Francisco, CA: ASP), 70  
 Sbarrato, T., Ghisellini, G., Giovannini, G., & Giroletti, M. 2021, *A&A*, **655**, A95  
 Shakura, N. I., Sunyaev, R. A., & Zilitinkevich, S. S. 1978, *A&A*, **62**, 179  
 Sikora, M., & Begelman, M. C. 2013, *ApJL*, **764**, L24

Silpa, S., Kharb, P., Harrison, C. M., et al. 2021, [MNRAS](#), **507**, 991  
Simpson, C., Mulchaey, J. S., Wilson, A. S., Ward, M. J., &  
Alonso-Herrero, A. 1996, [ApJL](#), **457**, L19  
Sobolewska, M. A., Siemiginowska, A., & Gierliński, M. 2011, [MNRAS](#),  
**413**, 2259

Ulvestad, J. S., Wrobel, J. M., Roy, A. L., et al. 1999, [ApJL](#), **517**, L81  
Wang, A., An, T., Guo, S., et al. 2023, [MNRAS](#), **523**, L30  
Wang, A., An, T., Jaiswal, S., et al. 2021, [MNRAS](#), **504**, 3823  
Wegner, G., Salzer, J. J., Jangren, A., Gronwall, C., & Melbourne, J. 2003, [AJ](#),  
**125**, 2373